Asian Journal of Agriculture and Biology
https://doi.org/10.35495/ajab.2026.01

Original Article

Modulatory effects of Rutin on inflammation and tumor progression in MCF-7-induced breast cancer in mice

Amira Ragab EL Barky[1], Tarek Mostafa Mohamed[1], Kamel Chaieb[2,3], Bochra Kouidhi[4], Ehab M. M. Ali[2*]

[1]Division of Biochemistry, Department of Chemistry, Faculty of Science, Tanta University, Tanta, Egypt
[2]Department of Biochemistry, Faculty of Science, King Abdulaziz University, Jeddah, Saudi Arabia
[3]Center of Artificial Intelligence in Precision Medicines, King Abdulaziz University, Jeddah, Saudi Arabia
[4]Laboratory of Analysis, Treatment and Valorization of Pollutants of the Environmental and Products, Faculty of Pharmacy, University of Monastir, Tunisia

**Corresponding author's email:* emali@kau.edu.sa
Received: 02 January 2026 / Revised: 16 March 2026 / Accepted: 27 March 2026 / Published Online: 09 April 2026

Abstract

Dysregulation of inflammatory and antioxidant signaling is characteristic of breast cancer development and influences therapeutic efficacy. This study investigated the relationship between inflammation and cancer invasion by assessing levels and/or gene expression of COX2, Adipoq, PPARγ, uPAR, sialic acid, and heparinase; apoptosis via caspase-3 evaluation; and redox balance in MCF-7 breast cancer mice treated with rutin. Three groups of virgin female mice were divided: (i) a control group; (ii) an MCF-7 group that was treated with Imuran before being injected with MCF-7 cells; and (iii) an MCF-7/rutin group that was given rutin (200 mg/kg). Biochemical and histological analyses were assessed after two and four weeks of post-treatment. Mice bearing breast tumors and treated with rutin exhibited less GATA-3 expression in mammary tissue at 4 weeks, signifying reduced cell invasiveness in mammary tissue at 4 weeks, Rutin therapy also resulted in decreased serum levels of prolactin, estrogen, and CA15-3 At two weeks, both untreated and rutin-treated tumor-bearing mice showed increased levels of COX2, uPAR and sialic acid, demonstrating higher inflammation and invasive potential. By four weeks, rutin-treated mice exhibited elevated serum sialic acid compared to control, but reduced compared with untreated mice, accompanied by elevated caspase-3, indicating enhanced apoptosis. Gene expression analysis revealed the upregulation of PPARγ at both 2 and 4 weeks and Adipoq at 2 weeks, suggesting the activation of apoptotic pathways and adipocyte differentiation. COX2 and heparinase were downregulated at both 2- and 4-weeks reflecting suppression of inflammation and invasion. Rutin-treated mice had reduced mammary MDA and nitric oxide levels at 2 and 4 weeks while mammary GSH and catalase activity were elevated at 2 weeks and depleted at 4 weeks in comparison to healthy mice. It was concluded that rutin treatment of mice bearing breast cancer improved oxidative balance, modulated inflammation, reduced invasion, and preserved mammary tissue structure in breast cancer-induced mice. It is recommended to study the treatment of mice with breast cancer or other types of cancer with chemotherapy combined with rutin to mitigate the side effects of these drugs.

Keywords: Rutin, Tumor breast markers, GATA-3, COX-2, Heparinase, PPARγ, Adipoq, NO, ROS

Graphical Abstract

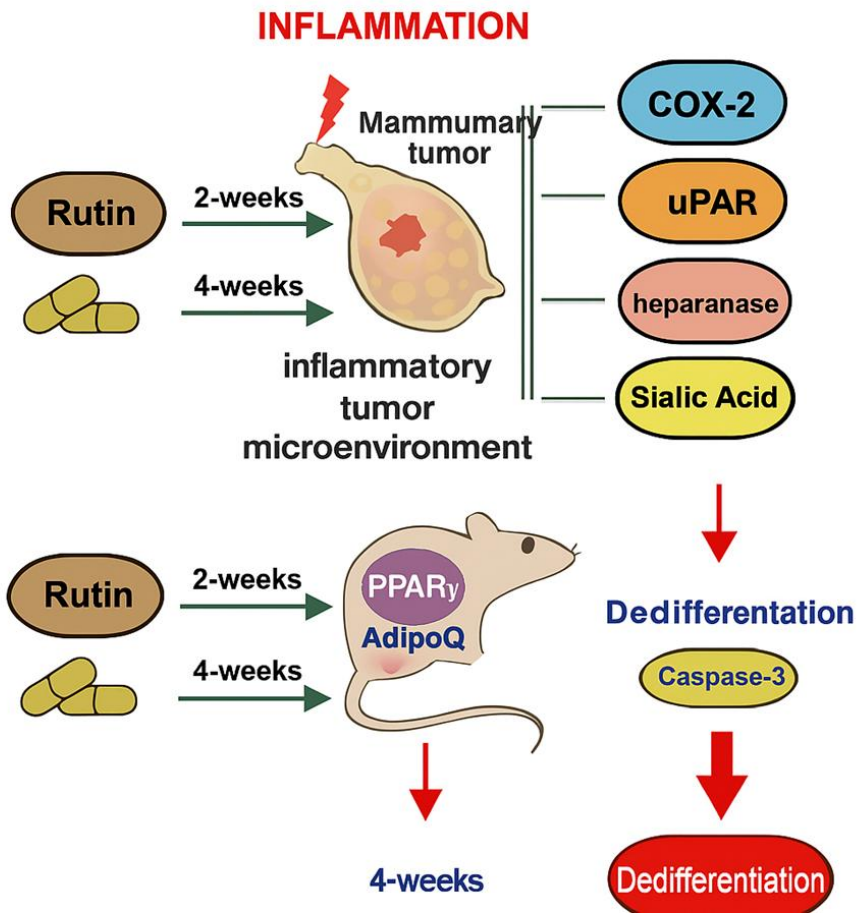

A diagram illustrates the interactions of breast cancer tumors in mice with inflammation, invasion, and apoptosis (COX-2, heparinase, sialic acid, adipoq/PPARγ, and caspase-3). Treatment with rutin implies potential regulatory effects on breast cancer.

How to cite this article:
EL Barky AR, Mohamed TM, Chaieb K, Kouidhi B and Ali EMM. Modulatory effects of Rutin on inflammation and tumor progression in MCF-7-induced breast cancer in mice. Asian J. Agric. Biol. 2026: e202601. DOI: https://doi.org/10.35495/ajab.2026.01

Introduction

Breast cancer remains one of the most prevalent cancers in women across the world, with high mortality and morbidity rates. International data indicate that breast cancer caused an estimated 2.3 million new cases and 670,000 deaths globally in 2022 (Kim et al., 2025, He et al., 2026). Tumor cell proliferation, angiogenesis, and invasion are stimulated by the inflammatory infiltration of immune cells and cytokine release in the tumor, thereby promoting tumor growth and metastasis (Nishida and Andoh, 2025). Inflammation stimulates both ROS and immune responses, leading to DNA damage and reducing apoptosis, and increases the body's resistance to treatment (An et al., 2024).

Although traditional therapies have improved, their low efficacy and toxicity mean more efficient and less toxic therapies are required. Traditional therapeutic systems rely on crude extracts of whole plants or their parts, such as *Neurada procumbens* and *Octhochloa compressa*, which have antioxidant, antimicrobial, and anti-inflammatory activities and treat chronic illnesses. *Neurada procumbens* has rich phytochemicals, antioxidant capacity, and antimicrobial activity. *Octhochloa compressa* has shown anti-inflammatory effects in both in vitro and in vivo models (Aslam et al., 2023a, 2023b, 2021). Natural substances, such as flavonoids, have the focus of their chemopreventive and anticancer activity. Flavonoids, including quercetin, apigenin, luteolin, genistein, and epigallocatechin gallate (EGCG), exert anticancer effects through induction of apoptosis, inhibition of angiogenesis, and suppression of tumor proliferation. Quercetin has inhibitory effects against breast cancer, while apigenin has potent activity against colorectal and breast cancers by regulating cell cycle progression and inducing apoptosis (Daneshvar et al., 2023; Wu et al., 2025). Genistein from soy has a role in the anticancer activity of breast cancer, and EGCG from green tea exhibits anticancer potential against lung, liver, breast, prostate, stomach, mammary gland, and colon based on preclinical data (Bhat et al., 2021; Singh et al., 2011).

Rutin, a glycosylated form of quercetin (quercetin-3-O-rutinoside), has a greater solubility and stability than the aglycone form because it is metabolically converted to quercetin in the body, which has been widely studied due to its antioxidant, anti-inflammatory, and anticancer properties (Bai et al., 2015; Gul et al., 2026). Rutin is a hydrophobic polyphenolic flavonoid chemical, and it is present in many plants such as buckwheat seeds, apricots, tea, cherries, grapes, grapefruit, onion, plums, and oranges (Bai et al., 2015; Gul, et al., 2026). Rutin is a non-toxic chemical compound derived from Ruta graveolens, which is also known as vitamin P or rutoside and can be described by its several biological activities (Tobar-Delgado et al., 2023). Reactive oxygen species, inflammation, and gene expressions associated with tumor proliferation are reduced by treating cancer cells with rutin (Akash et al., 2024; Alharbi et al., 2025). Rutin inhibited oncogenic Kras-driven tumorigenesis in Kras-mutant transgenic mice (Wang et al., 2025). Rutin enhanced apoptotic cell death by increasing the expression of proapoptotic genes (Bax, caspase-3, caspase 8, and caspase-9) and decreasing the gene expression of antiapoptotic protein Bcl-2 in pancreatic cancer cell lines (Huo et al., 2022). Rutin has significant neuroprotective effects because of its antioxidant, anti-inflammatory, anti-apoptotic, and anticonvulsant effects. It improves neural signaling and blood-brain barrier integrity (Chunmei and Shuai, 2025).

Rutin–zinc oxide nanoparticles (Rut–ZnO NPs) exert anticancer effects against chronic myeloid leukemia (CML) cells by promoting apoptosis through upregulation of Bax mRNA and downregulation of Bcl-2 expression (Alidoust et al., 2025). Rutin shows hypolipidemic and hepatoprotective effects in nonalcoholic fatty liver disease by reducing triglyceride accumulation and oxidative damage in lipid-laden hepatocytes (Liu et al., 2017). Serum HDL cholesterol level was raised, whereas VLDL and LDL cholesterol levels were reduced in diabetic rats (DR) treated with troxerutin. In addition, *peroxisome proliferator-activated receptor gamma* (*PPARγ*) gene expression was downregulated in adipose tissue of DR treated with troxerutin (Gul et al., 2026). Rutin enhances the efficacy of chemotherapeutic therapy of breast cancer and mitigates pirarubicin-induced cardiotoxicity (Li et al., 2026).

This study aimed to evaluate the therapeutic efficacy of rutin in mice bearing breast cancer induced by MCF-7, focusing on its effects on oxidative stress and inflammation responses. The study also examined the interrelations between biomarkers of inflammation, invasion, and apoptosis induced by breast tumor-bearing mice and the modulative effects of rutin administration after two and four weeks. To elucidate these triggering processes, biomarker profiling was achieved, including hormonal markers (estradiol,

https://doi.org/10.35495/ajab.2026.01

prolactin), tumor markers (CA15-3), and oxidative stress indicators (malondialdehyde (L-MDA), glutathione (GSH), nitric oxide (NO), inflammatory and invasive biomarkers cyclooxygenase (COX-2), (urokinase-type plasminogen activator (uPAR), heparinase and sialic acid). Additionally, gene expression levels of (COX-2, adiponectin (Adipoq), PPARγ, and heparinase were analyzed alongside histopathological and immunohistochemical evaluation of GATA Binding Protein 3 (GATA-3). The findings seek to better the understanding of rutin-based therapies with improved efficacy for breast cancer treatment.

Material and Methods

Experimental design of MCF-7-induced mammary tumors in azathioprine-treated Swiss albino mice

For this study, 45 female Virgin Swiss albino laboratory mice weighing 25 ± 3.0 g were used. Mice were purchased from a farm in Alexandria, Egypt. Animals were housed at 25 °C under a 12-hour light/dark cycle with unlimited access to water and a defined control diet, formulated to meet standard nutritional requirements and purchased from local supplements. The Faculty of Science at Tanta University in Egypt (ethics approval number: IACUC-SCI-TU-0527) upheld national ethical principles for laboratory animal care, and all procedures were performed in accordance with these guidelines (Rasheed et al., 2024; Gul et al., 2026). Mice were given a seven-day acclimatization period before the experiment commenced.

Cell culture of MCF-7

The Cell Culture Department of VACSERA (Cairo, Egypt) has sold MCF-7. The MCF-7 cells were cultured in a T-25 flask that contained 3 mL of complete RPMI 1640 medium from Gibco (with 10% deactivated fetal bovine serum albumin (FBS) from Biotechne Company and 1% penicillin-streptomycin 5000 U/mL from Thermo-Fisher Scientific Company). The flask was incubated for 24-48 hours at 37 °C in humidified 5% CO_2 / 95% air until the confluence reached 70-90%. After that, cells were detached by adding 1.5 mL of trypsin-EDTA for 5 minutes. Cells in suspension were centrifuged, and the pellets (cells) were grown in T-75 flasks in a CO_2 incubator. The preceding stages were repeated until the desired number of cells was obtained. The cells were counted using a hemocytometer after being stained with 0.4% trypan blue. For injection into the female nipple mice, cells have been harvested and resuspended in complete media (Ali et al., 2018; Plumb, 2004).

Azathioprine-induced immunosuppressed Swiss albino mice bearing MCF-7 breast carcinoma xenografts

Female Swiss albino mice weighed 25 ±3 g and were 6–8 weeks old, representing sexually mature young adults with intact estrous cycles; therefore, endogenous estrogen production was present throughout the experimental period. For tumor induction, 2×10^6 MCF-7 carcinoma cells suspended in sterile saline were injected orthotopically into each of the two fourth mammary nipples (one on each side) of the mice (Avril et al., 2019). No exogenous estrogen pellets were administered. Tumor establishment depended on high-density cell inoculation into the mammary fat pad. A total of forty-five mice were assigned to three primary experimental groups.

Group I (Normal group, n = 13) received saline instead of the immunosuppressive drug and did not undergo tumor induction.

Group II (MCF-7 group, n = 16) received oral azathioprine (Imuran; RPG Life Science Ltd., India) to induce immunosuppression prior to MCF-7 cell injection. Azathioprine was administered for two consecutive days at a dose of 10 mg/kg body weight suspended in olive oil (0.5 mL), followed by a third dose of 5 mg/kg body weight on the day of tumor cell injection (Avril et al., 2019; Al-Shahari et al., 2021).

Group III (MCF-7/Rutin group, n = 16) received the same azathioprine immunosuppression regimen as group II. Following immunosuppression, 2×10^6 MCF-7 cells were injected into each of the two fourth mammary nipples. Twenty-four hours after tumor cell inoculation, the mice were orally administered rutin daily at a dose of 200 mg/kg body weight for one month (Dixit, 2014).

Five mice from each group were anesthetized with ketamine, blood samples were collected, and the animals were sacrificed two weeks after MCF-7 cell injection, and the remaining animals were sacrificed after four weeks under ketamine anesthesia. At the end of the experiment, blood samples were collected from all mice, and serum was separated by centrifugation at 4000 rpm for 15 minutes. Mammary glands were

excised, and both normal and tumor tissues were immediately stored at −20 °C until further analysis.

Histological examination

Hematoxylin and eosin staining

Samples of the mammary glands were immediately fixed for 24 hours in 10% formalin. The samples were adequately cleansed, dried, and then embedded in paraffin wax (Afzal et al., 2024; Ali et al., 2024; Sikandar et al., 2020). The 5 µm segment was prepared. Dewaxed, rehydrated, and processed for hematoxylin and eosin staining (Fischer et al., 2008).

Immunohistochemical examination

To prevent nonspecific staining, the sections were dewaxed, rinsed in phosphate-buffered saline (PBS), incubated for 10 minutes with an aqueous solution of 0.3% hydrogen peroxide, and then washed twice in phosphate-buffered saline. The slices were incubated with the primary Gata-3 antibody (clone OCH1E5, dilution 1:600, DAKO, Carpinteria, CA) for 40 minutes. After washing, the slides were soaked in biotinylated secondary antibody, then washed one more time, and finally avidin-biotin. The slides were counterstained with Mayer's hematoxylin, dehydrated, and mounted after the reaction occurred with the addition of 3,3'-diaminobenzidine. The positively stained area is brown. The sections were examined and photographed. The percentages of the areas occupied by positive staining were computed using ImageJ software (Magaki et al., 2019; Cimino-Mathews, 2021).

Determination of serum prolactin, estradiol, CA15-3, COX2, uPAR sialic acid, heparinase and caspase-3 levels

Serum levels of prolactin, estradiol, and CA15-3 serve as biomarkers for breast cancer diagnosis and treatment monitoring. Serum levels of COX-2, urokinase-type plasminogen activator (uPAR), sialic acid, and heparinase are indicative of inflammatory responses and cancer cell invasion and metastatic spread. Caspase-3 activity is a biomarker of apoptotic processes. Serum levels of prolactin (CSB-E07280m), estradiol (CSB-E05109m), CA15-3 (CSB-E04772h), COX-2 (CSB-E12910m), uPAR (CSB-E07369m), sialic acid (CSB-E13811h), heparinase (CSB-EL010716MO), and caspase-3 (E0969, CSB-E06882m) were quantified using specific ELISA kits according to the manufacturer protocols.

Quantitative real-time PCR (qPCR)

RNA extraction

Total RNA was isolated from both normal and tumor breast tissues using the PureLink™ RNA Mini Kit (Thermo-Fisher Scientific, Cat. No. MAN0019346) following the manufacturer's protocol as described by Urbinati et al. (2016). Briefly, tissues were weighed, kept on ice, and homogenized in 2 mL of lysis buffer supplemented with 2-mercaptoethanol. Homogenization was achieved by vigorous up-and-down and twisting motions while simultaneously chopping the tissue with an RNase-free pestle to ensure complete lysis. The lysates were centrifuged at 1200 g for 30 seconds, and the 200 µL supernatant was mixed with 500 µL of 100% ethanol. Aliquots of up to 700 µL were loaded onto the spin column and centrifuged, with the flow-through discarded after each step. Sequential washes with Buffer 1 and Buffer 2 were performed, followed by centrifugation and removal of the flow-through. RNA was eluted by adding 40 µL of lysis buffer to the column. The purity and concentration of the extracted RNA were determined using a Nanodrop spectrophotometer at 260/280 nm (Gasior et al., 2025).

Synthesis of cDNA

Complementary DNA (cDNA) was synthesized from total RNA using the Applied Biosystems™ High-Capacity RNA-to-cDNA Kit (Thermo Fisher Scientific, Cat. No. 4387406), according to the manufacturer's instructions as described by Ali et al. (2014a). For each reaction, up to 5 µL of RNA sample containing 2 µg of RNA was mixed with 10 µL of 2× RT buffer mix and 1 µL of 20× RT enzyme mix, and the final volume was adjusted to 20 µL with nuclease-free DEPC-treated water. Reverse transcription was performed in a thermocycler under the following conditions: 37 °C for 60 minutes to allow cDNA synthesis, followed by 95 °C for 5 minutes to inactivate the reverse transcriptase enzyme, and finally held at 4 °C for at least 5 minutes. The concentration and purity of the synthesized cDNA were determined spectrophotometrically using a NanoDrop instrument at 260/280 nm. This protocol has been widely applied in molecular oncology studies to ensure reliable downstream gene expression analysis (Schmittgen and Livak, 2008).

Real-time PCR (qPCR)

Quantitative real-time PCR was performed using the Bio-Rad CFX96™ Real-Time PCR Detection System with SYBR™ Green PCR Master Mix (Thermo Fisher Scientific) as described by Ali et al. (2014b). Each reaction mixture contained 2 µL of cDNA (40 ng/µL), 5 µL of SYBR™ Green PCR Master Mix, 1 µL of each forward and reverse primer (10 pmol/µL), and 2 µL of nuclease-free water, in a final volume of 10 µL. All reactions were conducted in triplicate to ensure reproducibility.

Thermal cycling conditions were as follows: an initial denaturation and polymerase activation step at 95 °C for 2 minutes, followed by 40 cycles of denaturation at 95 °C for 15 seconds, annealing at 60 °C for 30 seconds, and elongation at 72 °C for 45 seconds. Gene-specific primers for COX-2, Adipoq, PPARγ, and Heparinase were used, with GAPDH serving as the housekeeping gene (primer sequences are listed in Table 1). Relative gene expression was calculated using the $2^{-\Delta\Delta CT}$ method (Schmittgen and Livak, 2008).

Table-1. Primers of COX-2, Adipoq, PPARγ, heparinase, and GAPDH.

Gene	Forward primer (/5 ———— /3)	Reverse primer (/5 ———— /3)
COX-2	CCTTCTCCAACGTGAGCTACTA	TCCTTCTCTCCTGTGAACTCCT
Adipoq	GGTCCTGATTGGATGTGCCA	ACTGGACTCACCCTGCAAAG
PPARγ	GGCTTGAACTGCATTGTCCC	AGGGAAACCCACGAAGACAC
Heparinase	CCTTGCTGTCCGATACCTTT	CTGCCTCATCACGACTTCTATC
GAPDH	TCACCACCATGGAGAAGGC	GCTAAGCAGTTGGTGGTGCA

Determination of serum and mammary L-MDA, GSH, nitric oxide levels, and mammary catalase activity

A 10% homogenate of mammary gland tissues was made in ice-cold saline. The amounts of L-MDA in the serum and mammary tissues were evaluated by adding 0.5 ml of 20% trichloroacetic acid to the serum and mammary homogenate to precipitate protein and centrifuging for 5 minutes at 3000 *xg*. One ml of thiobarbituric acid was added to 0.5 ml of the supernatant, and heated for 15 minutes to 100 °C. The absorbance of pink color was measured at 530 nm (El Barky et al., 2020). Levels of GSH in serum and mammary homogenate were also assessed by the amount of reduced glutathione in serum and mammary tissue, which was measured by reacting 5, 5'-dithiobis-2-nitrobenzoic acid (DTNP) with GSH at pH 8.2. Using different concentrations of known GSH to create a standard curve, the yellow color development was measured at 412 nm and calculated (Ellman, 1959). Additionally, the levels of serum and mammary nitric oxide were measured by converting nitrate to nitrite using cadmium. When the Griess reagent and nitrite combine, a pink hue is produced. To calculate the total nitrite, the absorbance was measured at 540 nm (Vodovotz, 1996). Mammary catalase activity has been measured also using the rate of H_2O_2 oxidation at 240 nm (Xu et al., 1997).

Statistical analysis

Statistical significance was determined using one-way analysis of variance (ANOVA) followed by Tukey's post-hoc test. Values of $p < 0.05$ were considered significant for all analyses, which were conducted using the Costas program.

Results

Following this study, two mice died: one from the MCF-7 group (Group II) and one from the MCF-7/Rutin-treated group (Group III). Visible inflammation was noted in the nipple region of the mice within a few days post-injection of MCF-7 cells. Morphological examination of the mammary glands revealed tumor development in untreated breast tumor–bearing mice (Figure 1). At two weeks following MCF-7 cell injection, mice exhibited nodular tumors with limited hemorrhage (Figure 1a). By four weeks, these nodules showed increased hemorrhage (Figure 1b). Rutin-treated mice demonstrated improvements after two weeks of treatment (Figure 1c), and by four weeks, rutin administration resulted in the absence observable hemorrhage (Figure 1d).

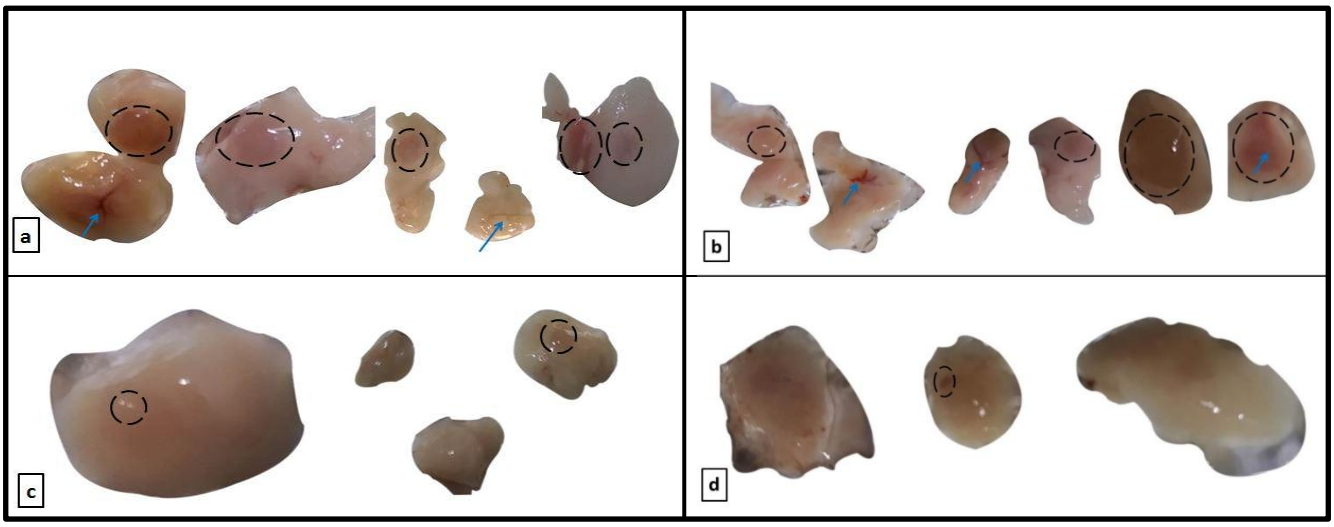

Figure-1. Morphology of mammary glands in breast tumor-bearing mice without or with rutin treatment, (a) 2 weeks after MCF-7 injection showing nodular tumor growth with focal hemorrhagic areas. (b) 4 weeks after injection showing more development tumor nodules and more observed hemorrhage (c) rutin treatment for 2 weeks showing fewer and less nodule relative to untreated (d) rutin treatment for 4 weeks showing a markedly reduced tumor nodules compared to the untreated, with no obvious hemorrhage.
Note: Arrows indicate hemorrhagic foci; dotted circles outline the boundaries of tumor nodules.

Histological examination

Hematoxylin and eosin staining

In healthy mice, the mammary tissue demonstrates tissue architecture, characterized by organized acini and ducts surrounded by peri-acinar and periductal fibrous tissue, embedded within an adipoblast-rich stroma (Figure 2a). Mice bearing breast cancer after two weeks exhibited proliferating anaplastic cells with hyperchromatic nuclei, loss of polarity, and marked pleomorphism accompanied by areas of hemorrhage (Figures 2b,c,d). After two weeks of rutin treatment, mammary sections demonstrated histological improvement, including reduced stromal vascular congestion, mild periductal fibrosis, partial restoration of epithelial stratification in some lactiferous ducts, and a decreased density of anaplastic cells (Figures 2e,f). By four weeks, untreated tumor-bearing mice showed stromal infiltration by tumor cells, dense adipose tissue, and focal hemorrhage (Figure 2g,h,i,j), whereas rutin-treated mice exhibited attenuated tumor cell infiltration, stromal integrity, regeneration of bundled collagen fibers, preservation of adipocyte and ductal morphology, and overall improved tissue organization (Figure 2k,l,m).

https://doi.org/10.35495/ajab.2026.01

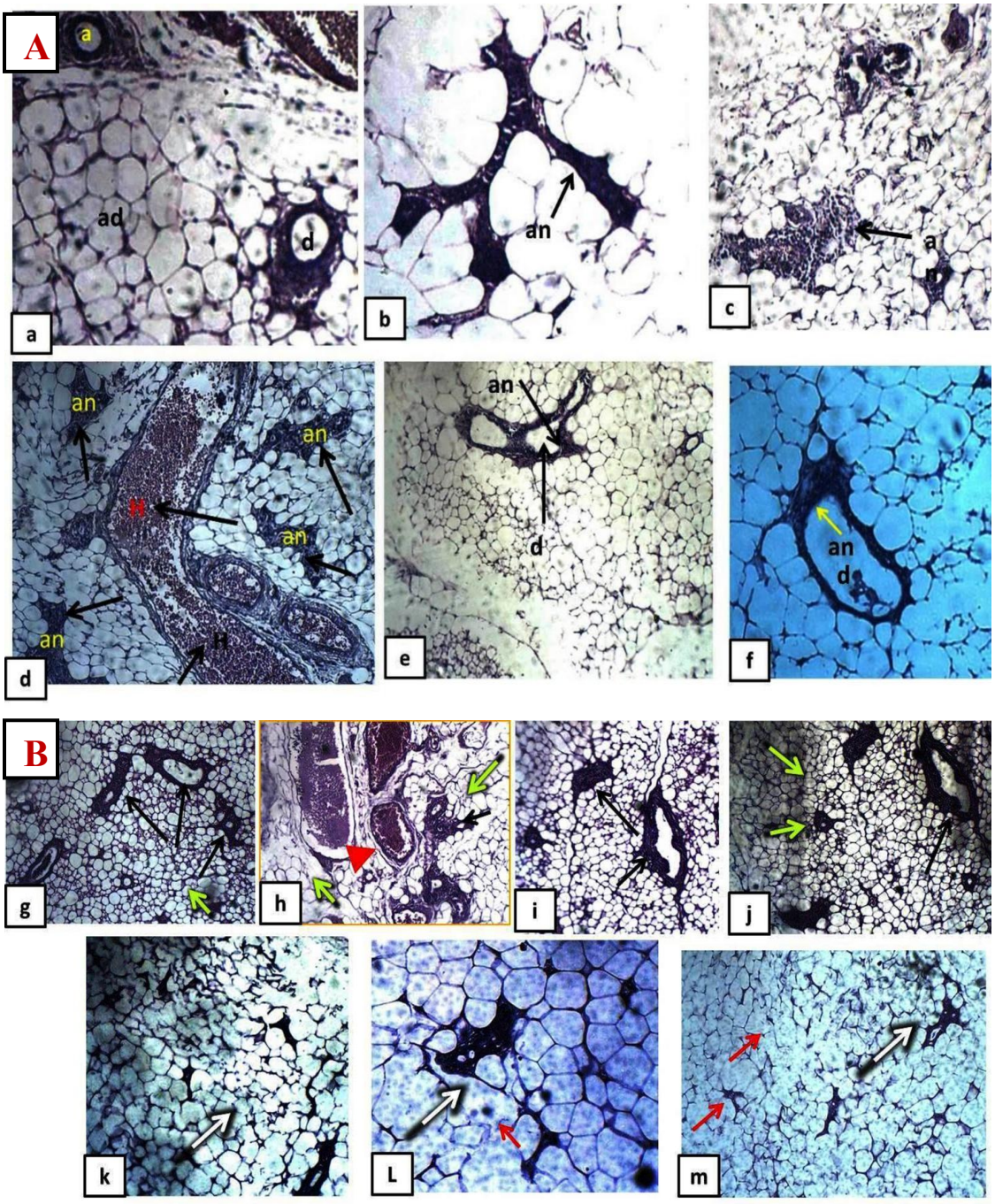

Figure-2. Photomicrographs of hematoxylin and eosin (H&E)-stained sections of mouse mammary glands (A) Represented control healthy mouse (a); mice bearing breast cancer (b, c, d) and mice bearing breast cancer treated with rutin (e, f) after two weeks. (B) Represented mammary sections from mice bearing breast cancer (g, h, i, j) and mice treated with rutin after four weeks (k, l, m).

(A) Normal histological architecture of healthy mouse indicated periacinar/periductal fibrous tissue embedded within adipoblasts (ad) (well-organized acini a, ducts d) of healthy mouse (Figure 3a), mice bearing breast cancer shows proliferating anaplastic cells (an) (Figure 3b,c,d) with hyperchromasia, loss of polarity, pleomorphism, and occasional mitotic figures, replacing acinar and ductal structures focally, accompanied by areas of hemorrhage (Figure 3d). Mice treated with rutin demonstrates histological improvement, including reduced stromal vascular congestion, mild periductal fibrosis, stratification of the epithelial lining in some lactiferous ducts (d), and fewer anaplastic cells (an) (Figure 3e,f) (H&E, ×200).

https://doi.org/10.35495/ajab.2026.01

(B) Mice bearing breast cancer exhibits tumor cells infiltrating the stroma, density of adipose tissue with anaplastic cells (Figure 3g,h,i,j). and focal hemorrhage/necrosis**)** (Figure 3h). Mice treated with rutin shows tumor cell infiltration with histological improvement (Figure 3k,l,m) (H&E, ×200).

Immunohistochemical examination

In this study, immunohistochemical analysis showed that GATA-3 was nuclear stained in untreated mice bearing breast cancer and can be used in the diagnostics of breast cancer. GATA-3 is a transcription factor for the luminal cell differentiation and is generally considered a sensitive ductal and lobular carcinoma biomarker, which can be detected to identify malignant cells. GATA-3 expression in mammary glandular epithelium revealed minimal staining in normal healthy mice (Figure 4a), with only 0.22% of cells. The mammary tissues from breast cancer–bearing mice exhibited a marked increase in GATA-3-positive cells, reaching 26.26% and 57.14% at the 2- and 4-week periods in Figure 3 (b, c, d), indicating tumor cell proliferation and stromal infiltration. Rutin-treated mice showed a reduction in GATA-3 expression, with 10.43% and 8.45% of cells staining positively at 2 and 4 weeks (Figure 3 (e,f)), indicating attenuation of tumor-associated GATA-3 expression.

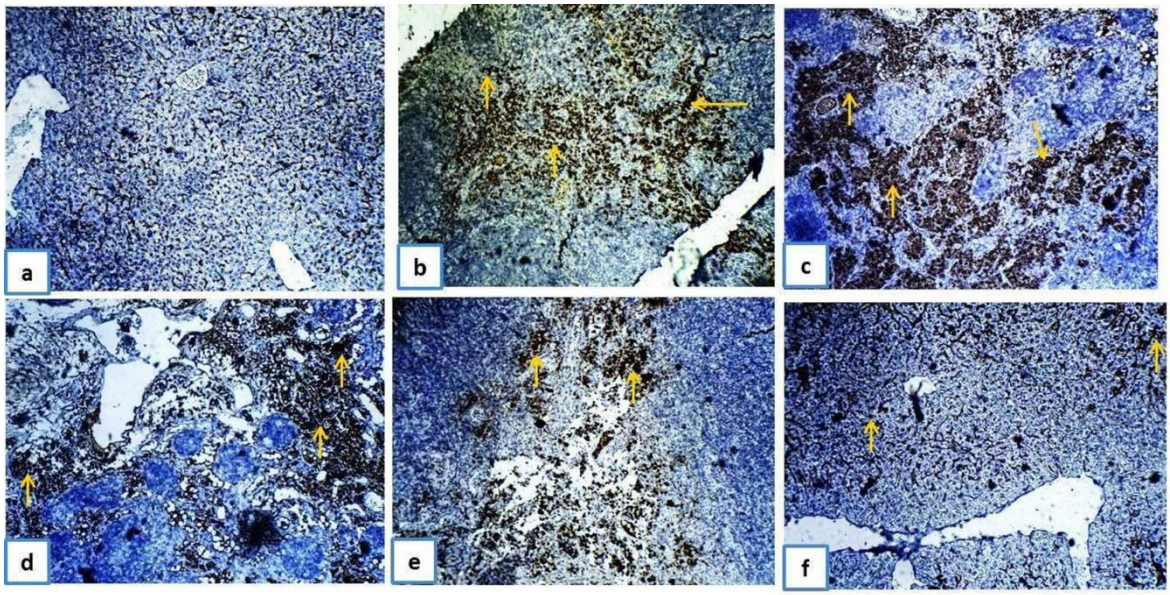

Figure-3. Immunohistochemical photomicrographs illustrate GATA-3 expression in mouse mammary glands. Control mammary tissue (a), shows normal glandular epithelium. Mammary tissue from mice bearing breast cancer (b), (c), (d) show widespread and intense GATA-3 staining (yellow arrows) consistent with tumor cell proliferation and stromal infiltration. GATA-3 staining is localized with reduced shows in mice bearing breast cancer and treated with rutin (e, f) indicating attenuation of tumor-associated GATA-3 expression (×200).

Serum prolactin, estradiol, CA15-3, COX-2, uPAR, sialic acid, heparinase and caspase-3 levels

The levels of serum estradiol and prolactin were significantly increased after two weeks of tumor induction ($p<0.001$) compared to healthy mice. Serum prolactin and estradiol levels in mice bearing tumors and treated with rutin were 2.5-fold and 2.1-fold higher ($p<0.001$), respectively, compared to normal mice. By the fourth week, prolactin and estradiol levels in the mice treated with rutin showed a modest increase ($p<0.05$), whereas changes in the mice bearing breast cancer were statistically non-significant (Figures 4a, b). Serum CA15-3 levels were significantly elevated in MCF-7-induced mice at both two and four weeks ($p<0.001$) compared to the normal mice. Mice treated with rutin demonstrated a marked reduction in CA15-3 levels ($p<0.001$) compared to mice bearing breast cancer, although values remained above those of normal mice (Figure 4c).

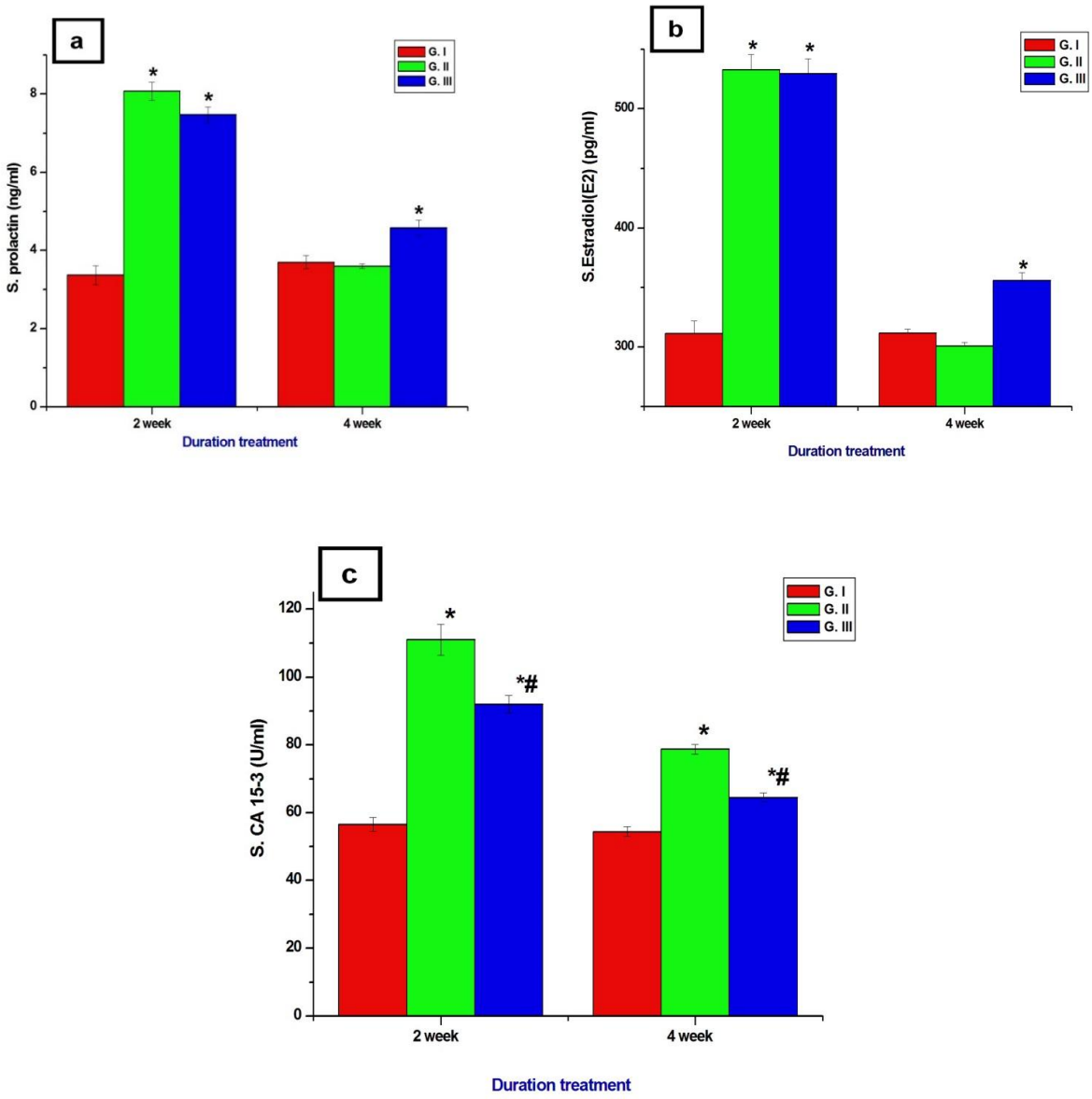

Figure-4. Serum prolactin, estradiol, and CA 15-3 levels (a,b,c respectively) in mice bearing breast cancer treated with rutin at 2 and 4 weeks. Data are presented as mean ± SD (n=5).
* indicates a significant difference compared to the control at $p < 0.001$
# indicates a significant difference compared to the untreated MCF-7 group (G.II) at $p<0.001$.

Serum COX-2 and uPAR levels were significantly increased in both the MCF-7 and MCF-7/Rutin groups during the two weeks ($p<0.001$), compared to controls. However, no significant changes were observed in either group (GII & GIII) after the two weeks (Figure 5a, b). After four weeks, serum sialic acid level was significantly elevated ($p<0.001$) in the MCF-7 group compared to healthy mice. The MCF-7/Rutin group exhibited significantly lower levels ($p<0.001$) than the MCF-7 group, though these did not return to baseline values observed in normal mice (Figure 5c).

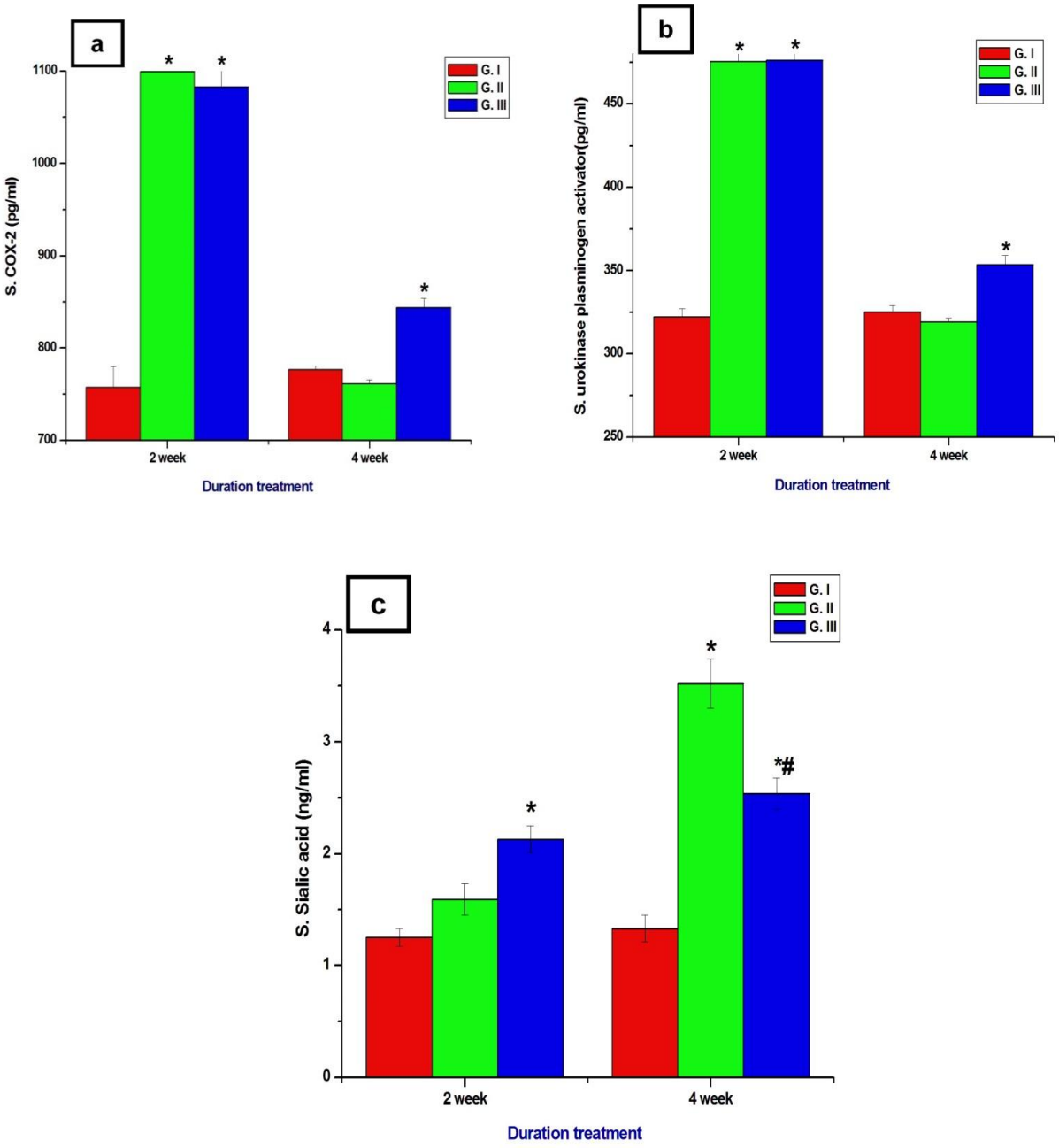

Figure-5. Serum COX-2, uPAR, and sialic acid levels (a,b.c respectively) in mice bearing breast cancer treated with rutin at 2 and 4 weeks. Data are presented as mean ± SD (n=5).
* indicates a significant difference compared to the control at $p < 0.001$
# indicates a significant difference compared to the untreated MCF-7 group (G.II) at $p<0.001$.

Serum heparinase levels were significantly increased ($p<0.001$) in the MCF-7 mice group after four weeks compared to healthy controls. The MCF-7/Rutin group after four weeks showed a significant reduction ($p<0.001$) in heparinase levels compared to the MCF-7 group, with a significant increase ($p<0.001$) compared to normal mice (Figure 6a). Serum caspase-3 levels were significantly elevated ($p<0.001$) in the MCF-7 group compared to both the control and MCF-7/Rutin groups ($p<0.001$) after two weeks. This

elevation was markedly reduced in the MCF-7 group ($p<0.001$) by the fourth week and elevated ($p<0.001$) in the MCF-7/Rutin group (Figure 6b).

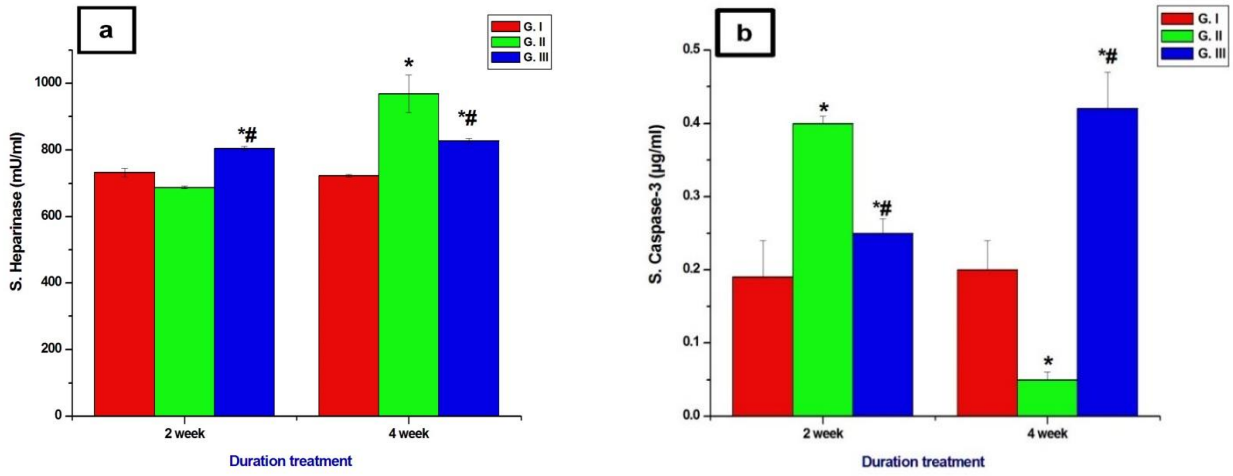

Figure-6. Serum heparinase and caspase-3 levels (a, b) in mice bearing breast cancer treated with rutin at 2 and 4 weeks. Data are presented as mean ± SD (n=5).
* indicates a significant difference compared to the control at $p < 0.001$
# indicates a significant difference compared to the untreated MCF-7 group (G.II) at $p<0.001$.

Gene expression of COX2, ADQ and PPARγ and heparinase

The data demonstrates a significant downregulation of COX2 and heparinase mRNA expression ($p<0.001$) in the mammary tissue of both the mice bearing breast cancer and the rutin-treated when compared with the normal control. In mice treated with rutin for two weeks, the expression levels of COX 2 and heparinase were elevated compared to mice bearing breast cancer ($p<0.001$) but were still significantly reduced ($p<0.001$) compared with the untreated (Figure 7a and d). Adipoq and PPARγ expressions were upregulated ($p<0.001$) in two weeks in mammary tissues of mice bearing breast cancer. Adipoq expression declined ($p<0.001$) in the four weeks, while PPARγ remained elevated ($p<0.001$). In the MCF-7/Rutin-treated group, both Adipoq and PPARγ showed sustained upregulation in two and four weeks (Figures 7b and c).

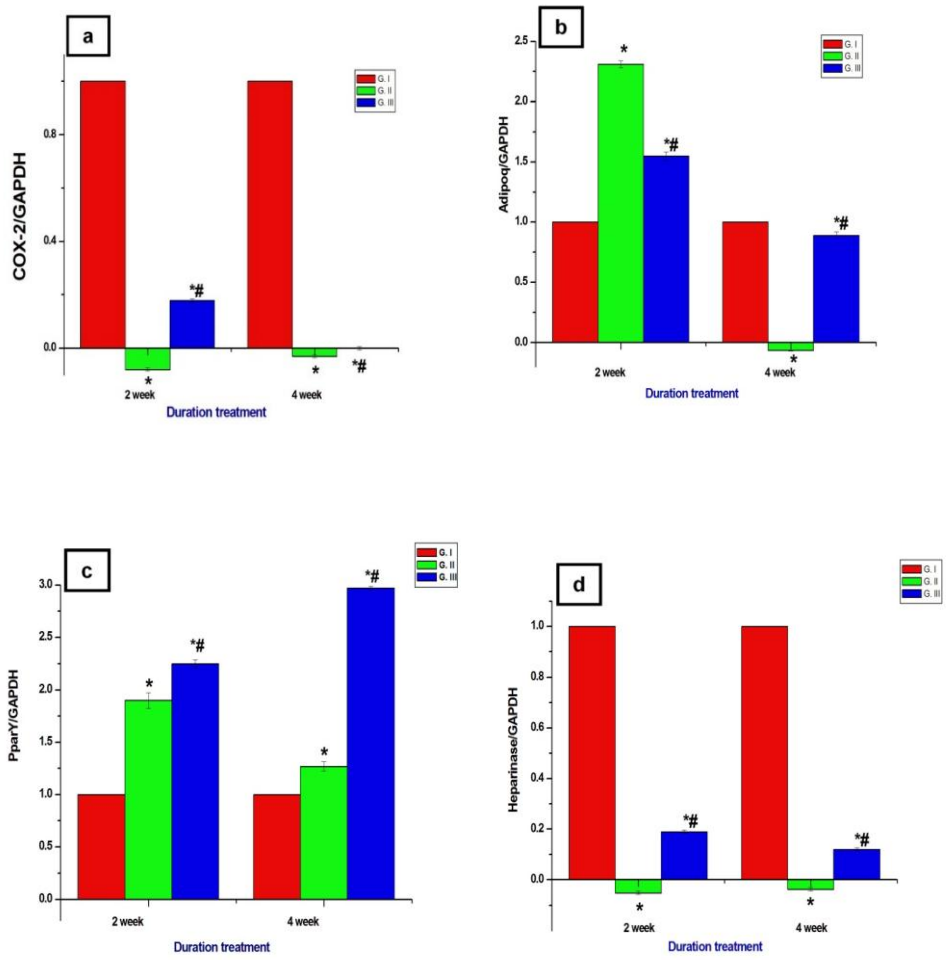

Figure-7. Fold change in mRNA expression of COX2, Adipoq, PPARγ, and heparinase in mammary tissues of breast cancer-induced mice treated with rutin. Gene expressions were quantified by qRT-PCR and normalized to GAPDH. Data are presented as mean ± SD (n=5).

* indicates a significant difference compared to the control at $p < 0.001$

# indicates a significant difference compared to the untreated MCF-7 group (G.II) at $p<0.001$.

Serum and mammary L-MDA, GSH, nitric oxide levels and mammary catalase activity. Serum L-MDA levels were significantly elevated ($p<0.001$) in both the MCF-7 and MCF-7/Rutin groups at two and four weeks compared to the normal mice. Mammary L-MDA levels were significantly reduced ($p<0.001$) in these groups. After 4 weeks, the MCF-7/Rutin group exhibited lower ($p<0.001$) mammary L-MDA levels than the MCF-7 group (Figures 8a and b). Serum GSH levels were significantly decreased in both the MCF-7 and MCF-7/Rutin groups at 2 and 4 weeks as compared to the normal control. Mammary GSH levels were significantly elevated ($p < 0.001$) in the MCF-7 group after 2 weeks but returned to near-control levels in the MCF-7/Rutin group by week 4. At this time, mammary GSH levels in the MCF-7/Rutin group were significantly lower ($p<0.001$) than those in the MCF-7 group (Figures 8c and d).

https://doi.org/10.35495/ajab.2026.01

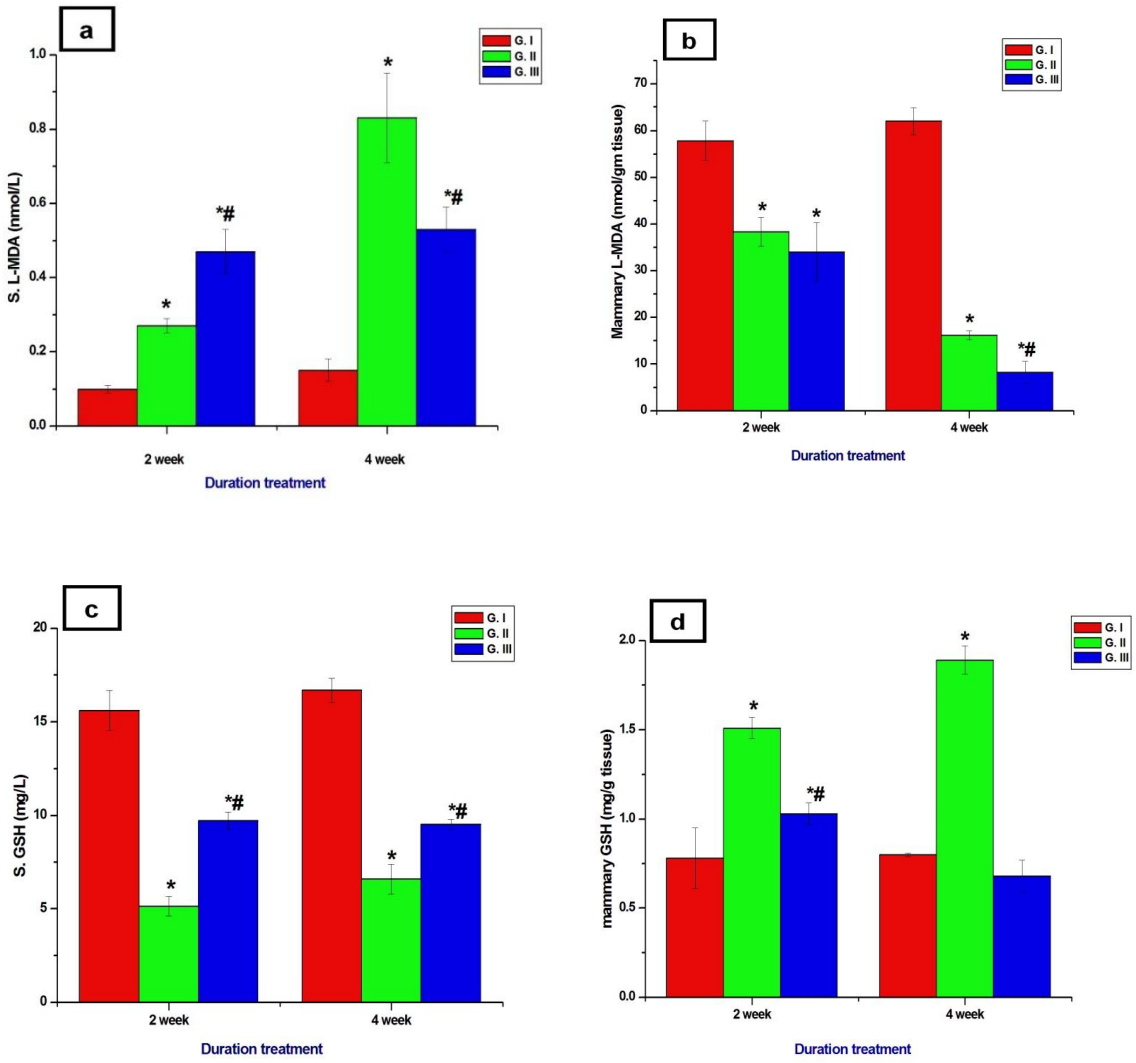

Figure-8. Serum and mammary L-malondialdehyde (MDA), (a, b) and glutathione (GSH) (c,d) levels of oxidative stress and antioxidant biomarkers levels in mammary tissues of breast cancer-induced mice treated with rutin at 2 and 4 weeks. Data are presented as mean ± SD (n=5).

*indicates a significant difference compared to the control at p< 0.05

# indicates a significant difference compared to the untreated MCF-7 group (G.II)) at p<0.001.

Serum nitric oxide (NO) level in the MCF-7 group showed a significant increase (p<0.001) after two weeks, then it significantly decreased after four weeks. In contrast, the MCF-7/Rutin group exhibited a significant elevation (p<0.001) in serum NO levels in 4 weeks compared to the MCF-7 group. Mammary NO levels were significantly reduced in both the MCF-7 and MCF-7/Rutin groups at 2 weeks relative to normal control. However, in 4 weeks, the MCF-7/Rutin group showed a significant increase (p<0.001) in serum NO compared to the MCF-7 group (Figures 9a and b). Mammary catalase activity was elevated (p<0.001) in the MCF-7 group for 2 weeks but significantly declined (p<0.001) by 4 weeks compared to normal mice. The MCF-7/Rutin group showed a significant reduction (p<0.001) in catalase activity for 2 weeks, followed by a notable increase at 4 weeks compared to the MCF-7 group (Figure 9 c).

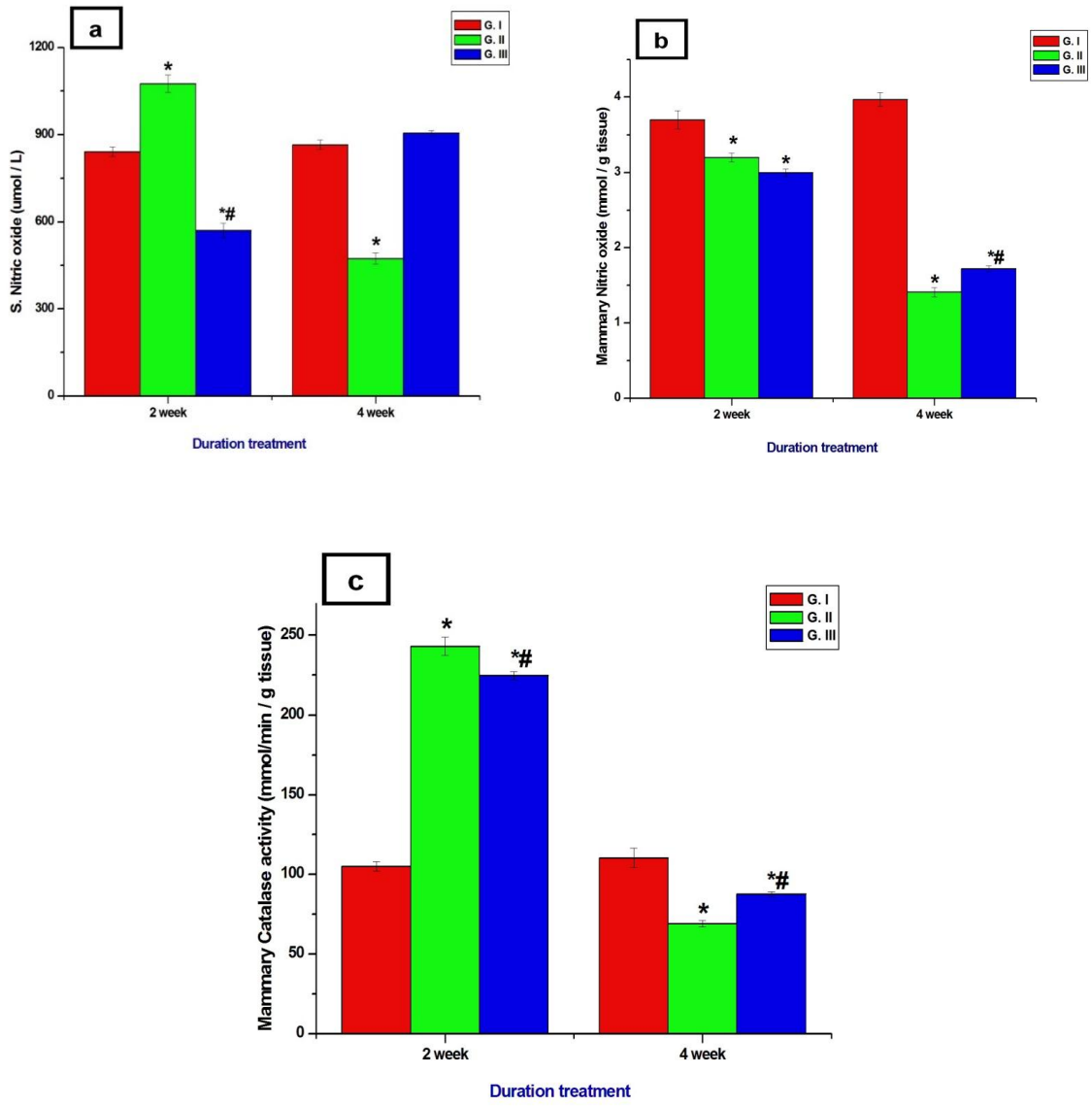

Figure-9. Serum and mammary nitric oxide levels (a,b) and mammary catalase activity (c) in breast cancer-induced mice treated with rutin at 2 and 4 weeks. Data are presented as mean ± SD (n=5.)
*indicates a significant difference compared to the control at p< 0.05
# indicates a significant difference compared to the untreated MCF-7 group (G.II)) at p<0.001.

Discussion

Cancer develops through the accumulation of genetic and epigenetic alterations that uncontrollably proliferate cells and disrupt tissue organization. Mutations or activation of oncogenes, inactivation of tumor suppressor genes, and apoptotic and DNA repair pathways are central to developing cancer (Ali et al., 2014b; Dupain et al., 2016). These alterations arise from environmental carcinogens, inherited susceptibility, and replication errors and accumulate through a multistep process that converts a normal cell into a malignant, invasive tumor (Brown et al., 2023). To create xenograft models, human-derived tumors should be implanted at specific sites in highly immunocompromised animals because they can destroy the produced cancer cells, therefore preventing the development of tumors. Subcutaneous injection of MCF-7 cells into immunosuppressed mice without estradiol enabled partial immunodeficiency,

permitting tumor engraftment and histologically confirmed growth after three weeks (Gorbushin et al., 2025). Azathioprine (Imuran) has been used to reduce the immune system of Swiss albino mice and prevent organ rejection in the post-transplant mice (Molyneux et al., 2008).

Natural products provide complementary therapeutic potential in the treatment of cancer because they contain diverse bioactive compounds with low toxicity and the ability to act on cellular pathways. These compounds include polyphenols such as curcumin and resveratrol, terpenoids like paclitaxel and artemisinin, alkaloids such as vincristine and berberine and flavonoids such as quercetin and kaempferol (Abbasi et al., 2025). Rutin has previously been shown to exert improved biochemical effects in tumor-bearing animal models. Dixit (2014) demonstrated that oral administration of rutin at 200 mg/kg and 400 mg/kg body weight, given three times weekly for 16 weeks, produced marked improvements in mice with DMBA-induced skin tumors. At these dose levels, rutin significantly reduced liver function biomarkers (ALT, AST, and ALP), enhanced key antioxidant enzyme activities (SOD, catalase, and GSH), and suppressed lipid peroxidation. It also has therapeutic effectiveness in many types of cancers, such as neuroblastoma, breast cancer, colon cancer, colorectal cancer, leukemia, hepatocellular carcinoma, and pulmonary metastases (Maugeri et al., 2023).

Mice bearing breast tumors in our study showed inflammation, hemorrhagic nodules, and mammary tissue overgrowth, poorly differentiated, with stromal degeneration, adipose distortion, and hyperchromatic nuclei. In contrast, rutin treatment improved stromal integrity and adipocyte and ductal preservation, demonstrating its ability to alleviate mammary tumors in mice induced by MCF-7. Rutin prevents angiogenesis, decreases cell proliferation, and enhances stromal remodeling in models of breast cancer, which induces apoptosis and cell cycle arrest in MCF-7 cells, inhibits angiogenesis through VEGF, and alters signaling pathways, including PI3K/Akt and MAPK (Lin et al., 2012). Rutin inhibits angiogenesis, reduces proliferation, and enhances stromal remodeling, contributing to improved tissue architecture and reduced malignancy in breast cancer models (Tejwan et al., 2022; Satari et al., 2021). GATA-3 is functional in the regulation of proliferation, differentiation, and epithelial-mesenchymal transitions that could affect metastatic ability and therapeutic efficacy (Mehra et al., 2005). GATA-3 is a transcription factor for the luminal nuclear cell differentiation and can be used as a sensitive biomarker for ductal and lobular breast carcinomas and can be detected in the nucleus to identify tumor cells. GATA-3 is more sensitive than other mammaglobin and GCDFP15, specifically in estrogen receptor (ER)-positive and luminal subtypes, but also useful in triple-negative and Estradiol and prolactin stimulate ER+ tumor cells and breast cancer progression by enhancing tumor cell movement, blood vessel formation, and growth. (Kavarthapu and Dufau, 2022).

Both serum estradiol and prolactin levels were highly increased after two weeks of tumor induction. The elevated estrogen and prolactin levels increase the levels of sphingosine-1-phosphate via upregulation of sphingosine kinase-1 or the JAK2/STAT5 pathway, which increases the proliferation and survival of tumor cells (Schuler and O'Leary, 2022; Hammer and Diakonova, 2024). The level of prolactin was increased after two weeks, and these results indicated that they played a dual role in stimulating tumour formation and early growth, and prolactin may have inhibited metastasis (Nouhi et al., 2006). Furthermore, prolactin also plays a role in resistance to the microtubule-targeting chemotherapeutics, including paclitaxel, by survival pathways (Čermák et al., 2020). Nevertheless, the administration of rutin could alleviate this resistance, and it can be a safer adjunct therapy, potentially enhancing the effectiveness of treatments like paclitaxel in breast cancer management (Ganeshpurkar and Saluja, 2017).

Serum CA15-3 is a human breast cancer biomarker; however, in our study, it was detectable in mice. CA15-3, derived from the extracellular N-terminal of MUC1, that becomes overexpressed, hypoglycosylated, and circulates in cancer. (Mukherjee et al., 2003). The high serum CA15-3 level detects breast cancer, which is associated with the progression and metastasis of the tumor (Duffy et al., 2000). The CA15-3 level was elevated in mice bearing breast cancer at both 2 and 4 weeks, whereas treatment with rutin showed a reduction compared to mice bearing breast cancer. CA15-3 is used for breast cancer screening or routine postoperative surveillance; it can be used in the treatment response and monitoring of metastatic disease. CA15-3 is associated with estrogen receptors and metastasis (Keshaviah et al., 2007; Uygur and Gümüş, 2021).

Inflammation promotes breast cancer by triggering cytokines, prostaglandins, free radicals, and growth

factors that cause mutations, epigenetic changes, and protein modifications, which disrupt cellular homeostasis, resulting in carcinogenesis (Nishida and Andoh, 2025). Serum COX2 and uPAR levels showed a significant elevation during two weeks in both untreated tumor-bearing mice and mice treated with rutin, compared with normal mice. It is suggested that early activation of inflammatory and proteolytic pathways linked to tumor growth and invasion inhibit apoptosis, promote angiogenesis through VEGF stimulation, and enhance metastatic potential. There were no significant differences in the serum COX2 level in the mice bearing breast tumors or after treatment with rutin. Routine treatment of mice bearing tumors at high doses may raise inflammatory biomarkers (Bell et al., 2022; Hajimehdipoor et al., 2023). COX2 mRNA was downregulated in both the mice bearing breast cancer and those treated with rutin compared with controls. After two weeks of rutin administration, COX2 levels increased relative to the untreated MCF 7 group but remained significantly below control levels.

Rutin has been shown to suppress inflammatory cytokines and downregulate COX-2 expression in cancer cells. After two weeks of rutin administration, COX-2 levels increased compared to the untreated MCF-7 group but remained significantly lower than those observed in the control group. Rutin demonstrates the ability to reduce COX-2 activity in cancer and inhibiting cytokine production (Hajimehdipoor et al., 2023). The differences between decreased gene expression of COX2 mRNA in the mammary glands of mice bearing breast cancer and elevated serum COX2 levels are consistent with that the biomarker COX 2 protein levels are better than mRNA levels in breast cancer (Sicking et al., 2014; Berbecka et al., 2021).

Both vascular endothelial growth factors (VEGF) and fibroblast growth factors (bFGF), which influence angiogenesis, tumour growth and spread, are bound to heparan sulphate (HS), which controls the release of these growth factors by heparinase. Serum heparinase level was increased after four weeks in MCF 7-bearing mice (Figure 7d). This result is consistent with data showing that patients and models of breast cancer have higher levels of heparinase and these growth factors (Sun et al., 2017; Jayatilleke and Hulett, 2020; Jayatilleke et al., 2023). In tumour-bearing mice, rutin treatment significantly decreased serum sialic acid and heparinase levels compared to healthy mice. Additionally, rutin decreased the expression of heparinase mRNA. Increased quercetin levels in cervical cancer cells are associated with decreased expression of mRNA and heparinase protein after 72 hours of incubation of rutin-treated cells (Zhang et al., 2013). Rutin may minimise the activation of PI3K/Akt pathways in MCF-7 cells triggered by heparinase (Riaz et al., 2013, Gopalakrishna et al., 2023).

The adipogenic and metabolic regulators seem to be upregulated in tumour tissue at early stages, which could be due to the efforts of the stroma to counteract malignant progression by ensuring differentiation and establishing anti-inflammatory conditions. As well as rutin being conserved both early and in later stages, the compound has the potential to maintain a differentiated metabolic microenvironment (Cheng et al., 2021). Mammary tissues from tumour-bearing mice showed increased mRNA expression of Adipoq and PPARγ at two weeks. By four weeks, Adipoq levels declined, while PPARγ remained elevated. In contrast, MCF 7/Rutin treatment upregulated both Adipoq and PPARγ at two and four weeks, which may be signifying a stimulatory effect on these adipogenic markers. The tumor cells become more susceptible to apoptosis, thus playing a role in decreasing the tumor burden and invasive capacity (Alharbi et al., 2025). An increase in apoptotic activity was indicated by elevated caspase 3 levels in mice treated with rutin. The integration of inflammation, invasion, metabolism, glycosylation, and apoptosis under the influence of rutin is an indicator of the change of differentiation and apoptosis. (Elbeltagi et al., 2025).

The loss of antioxidant defences and an increase in free radical production promote tumor development through genetic alterations (Hussain et al., 2025; Alam et al., 2025). Oxidative damage disrupts metabolic pathways, facilitating the development of neoplasms through free radical-mediated DNA damage (Reuter et al., 2010). Serum malondialdehyde (L-MDA) was higher in mice induced with breast cancer and treated with rutin in two and four weeks. Tumor-bearing mice had significantly lower L-MDA concentrations in the mammary tissue, particularly after the rutin treatment, when compared with those in circulation. In week four, rutin also decreased breast L-MDA, which suggests that the local antioxidant defence system, which may be mediated by enzymatic scavengers, alleviated lipid damage at the cancer site (Uti et al., 2025). Glutathione (GSH) represents redox equilibrium modulator in cancer. Systemic depletion or diminished synthesis of GSH is accompanied by chronic oxidative stress in tumors (Traverso et al.,

2013). GSH temporarily elevated in breast cancer – induced mice at two weeks to overcome elevated levels of ROS but thereafter declined. When mice were treated with rutin, the levels of mammary GSH dropped to lower levels than the ones of the untreated mice at the week four mark, which coincided with a decline in L-MDA, suggesting effective ROS neutralization or switching to other antioxidant systems. We show that rutin modulates GSH homeostasis, and thereby in repairing the glutathione-dependent redox cycles (Yang et al., 2012).

Nitric oxide (NO) action depends on the context in terms of being tumoricidal or tumor-promoting in terms of concentration and distribution. NO has effects on angiogenesis, apoptosis, cell cycle, invasion, and metastasis, and reactive nitrogen species play a role in inflammation and chronic oxidative stress that may lead to carcinogenesis (Andrabi et al., 2023). Serum NO level was elevated in mice bearing breast cancer after two weeks, then it reduced after four weeks. Tumor cells may increase NO consumption or inhibit iNOS during the development of breast cancer (Flaherty et al., 2019). Routine treatment of mice bearing breast cancer had risen in serum NO of tumors compared to untreated tumors in four weeks. Rutin regulates NO pathways and has an antioxidant and anti-inflammatory effect (Youssef et al., 2022). The increase in NO with rutin treatment could correspond to the physiological signalling, increasing the endothelial functioning and immune surveillance, thus assisting its anticancer properties. The level of mammary tissue NO in both the mice bearing breast cancer and the rutin-treated mice after two weeks reduced when compared to the control, indicating that the depletion was early in the locality. It could be due to a decrease in the activity of endothelial nitric oxide synthase (eNOS) or an elevation in tumor cell consumption, which is associated with endothelial dysfunction and metastasis (Smeda et al., 2018). Rutin regulates the NO levels, and iNOS expression indicates that it may be used to remodel the tumor cells to a less developed state, which supports its use as an adjuvant therapy in breast cancer (Youssef et al., 2022).

The increase in catalase activity in breast cancer-bearing mice after two weeks may be due to increasing of reactive oxygen species (ROS) produced during the tumor development. To respond to oxidative stress, cancer cells tend to increase the levels of antioxidant enzymes, including catalase, to sustain the redox balance, which helps to ensure survival and growth (Glorieux et al., 2018). The catalase activity decreased, indicating that progressive tumors could weaken antioxidant defences due to long-term oxidative stress, distorted signalling, and epigenetic regulation of catalase expression four weeks later (Tian et al., 2026). The catalase activity was lower in mice treated with rutin for two weeks than in mice bearing breast cancer, which may be indicative that rutin initially inhibits the catalase activity by decreasing the production of ROS or by directly altering the antioxidant enzyme expression (Rathod et al., 2023). A significant increase in catalase activity was observed in four weeks in mice treated with rutin, which suggests that antioxidant defence activation was delayed by rutin's main action in maintaining the stability of redox-responsive mechanisms (Enogieru et al., 2018).

Conclusion

This study demonstrates that rutin administration in a mouse model of MCF-7–induced breast cancer was associated with several histological and biochemical changes. Histopathological analysis of breast cancer bearing mice treated with rutin showed a reduction in periductal fibrosis, and vascular congestion in mammary tissue. Additionally, reduced GATA-3 expression indicated diminished localized tissue invasion. Biochemically, rutin treatment was associated with reductions in serum prolactin, estradiol, and CA15-3 levels, as well as alteration of COX-2, uPA, and sialic acid. Increased caspase-3 activity and reduced heparinase expression at week 4 suggest a high level of apoptosis and a low level of invasiveness. Gene expression analysis showed upregulation of PPARγ at 2 and 4 weeks and upregulation of Adipoq at week 2. Improved oxidative homeostasis and endothelial function are indicated by decreased malondialdehyde, elevated glutathione levels & catalase activity, and restoration of serum NO in mice bearing breast cancer and treated with rutin. These findings suggest that rutin may influence inflammatory, apoptotic, metabolic, and oxidative stress pathways in a mouse model of breast cancer, supporting its potential incorporation into therapeutic preparations. Further research is elucidating the mechanism of action of rutin in tumor-bearing mice and evaluating its synergistic efficacy when combined with chemotherapy.

Acknowledgement
The authors gratefully acknowledge the financial support provided by the Deanship of Scientific Research (DSR), King Abdulaziz University, Jeddah, Saudi Arabia, under project number IPP:440-130-2025. We also extend our gratitude to all colleagues who offered technical assistance and support during this work.

Disclaimer: None.
Conflict of Interest: None
Source of Funding: This study was financially supported by the Deanship of Scientific Research (DSR), King Abdulaziz University, Jeddah, Saudi Arabia, under project number IPP:440-130-2025.

Ethical Approval Statement
The questionnaire and methodology for the present study were approved by National ethical guidelines for the care of laboratory animals according to the Faculty of Science, Tanta University, Egypt, (Ethics approval number: IACUC-SCI-TU-0527).

Contribution of Authors
EL Barky AR & Mohamed TM: Conceptualization, methodology, investigation, formal analysis, data curation, validation and writing–original draft.
Chaieb K: Investigation, formal analysis, writing–original draft and validation, review & editing.
Kouidhi B: Methodology, validation, writing—original draft and editing.
Ali EMM: Conceptualization, methodology, data curation, funding acquisition, writing, review & editing and supervision.

All authors read and approved the final draft of the manuscript.

References

Abbasi HA, Atif M, Anjum MN, Ahmad J, Wahab A and Shah SAA, 2025. Potential of plant bioactive compounds for the treatment of cancer. Futur. Biotechnol. 5: 18–27.

Afzal G, Ali HM, Hussain T, Hussain S, Ahmad MZ, Naseer A, Iqbal R, Aslam J, Khan A, Elsadek MF and Al-Munqedhi BM, 2024. Effects of sub-lethal concentrations of lindane on histo-morphometric and physio-biochemical parameters of Labeo rohita. PLoS One 19(7): e0304387.

Akash SR, Tabassum A, Aditee LM, Rahman A, Hossain MI, Hannan MA and Uddin MJ, 2024. Pharmacological insight of rutin as a potential candidate against peptic ulcer. Biomed. Pharmacother. 177: 116961–116972.

Alam S, Afzal G, Hussain R, Ali HM, Sami A, Malik RM, Jabeen R, Ataya FS and Li K, 2025. Estimation of median LC50 and toxicity of environmentally relevant concentrations of thiram in *Labeo rohita*. npj Clean Water 8(1): 9.

Alharbi HOA, Anwar S and Rahmani AH, 2025. The potential role of rutin, a flavonoid, in the management of cancer through modulation of cell signaling pathways. Open Life Science, 20: 20251181.

Ali EM, Elashkar AA, El-Kassas HY and Salim EI, 2018. Methotrexate loaded on magnetite iron nanoparticles coated with chitosan: Biosynthesis, characterization, and impact on human breast cancer MCF-7 cell line. Int. J. Biol. Macromol. 120: 1170–1180.

Ali HM, Urbinati G, Chapuis H, Desmaële D, Bertrand JR, Couvreur P and Massaad-Massade L, 2014a. Effects of siRNA on RET/PTC3 junction oncogene in papillary thyroid carcinoma: from molecular and cellular studies to preclinical investigations. PLoS One 9(4): e95964.

Ali HM, Maksimenko A, Urbinati G, Chapuis H, Raouane M, Desmaële D, Yasuhiro H, Harashima H, Couvreur P and Massaad-Massade L, 2014b. Effects of silencing the RET/PTC1 oncogene in papillary thyroid carcinoma by siRNA-squalene nanoparticles with and without fusogenic companion GALA-cholesterol. Thyroid 24(2): 327-338

Ali HM, Hussain S, Ahmad MZ, Siddique AB, Ali S, Mohiuddin M, Ehsan M, Nadeem M, Qayyum A, Hussain R and Khan I, 2024. Molecular identification of different toxinogenic strains of *Clostridium perfringens* and histo-pathological observations of camels died of per-acute entero-toxaemia. Heliyon 10(6): e27859

Alidoust FA, Zahmatkesh H, Rasti B, Zamani H, Mirpour M and Mirzaie A, 2025. Zinc oxide fabricated by rutin as potent anti-leukemia

nanostructure. Naunyn-Schmiedeberg's Arch. Pharmacol. 398: 7005–7015.

Al-Shahari EA, El Barky AR, Mohamed TM and Alm-Eldeen AA, 2021. Doxorubicin, L-arginine, or their combination as a prophylactic agent against hepatic carcinoma in mice. Environ. Sci. Pollut. Res. 28: 37661–37671.

An X, Yu W, Liu J, Tang D, Yang L and Chen X, 2024. Oxidative cell death in cancer: mechanisms and therapeutic opportunities. Cell Death & Disease, 15: 556.

Andrabi SM, Sharma NS, Karan A, Shahriar SMS, Cordon B, Ma B and Xie J, 2023. Nitric oxide: Physiological functions, delivery, and biomedical applications. Adv. Sci. 10: e2303259.

Aslam J, Shahzad MI, Ali HM, Dilbar GH, Ahmad FUD, Sadiq F, Locatelli M, Ashraf H and Farooq U, 2021. In vitro and in vivo anti-inflammatory potential of *Octhochloa compressa* extracts in carrageenan-induced rats.Pak.-Euro J. Med. Life Sci.4(4): 265–274.

Aslam J, Shahzad MI, Ali HM, Ramzan M, Ahmad FUD, Aleem MT, Minhas A, Hirad AH and Alarfaj AA, 2023a. A multidirectional phytochemical profiling, antimicrobial, antioxidant and toxicity studies of *Neurada procumbens L.*; a desert medicinal plant. J. King Saud Univ. Sci. 35(8): 102862.

Aslam J, Shahzad MI, Ali HM, Ramzan M, Ahmad FUD, Mustafa MZ, Iqbal RK, Hirad AH, Alarfaj AA and Danish S, 2023b. Antioxidant and anti-inflammatory potentials of aerial and floral parts of *Neurada procumbens* extracts: in vitro and in vivo studies. J. King Saud Univ. Sci. 35(7): 102822.

Avril P, Vidal L, Barille-Nion S, Le Nail LR, Redini F, Layrolle P, Pinault M, Chevalier S, Perrot P and Trichet V, 2019. Epinephrine infiltration of adipose tissue impacts MCF7 breast cancer cells and total lipid content. Int. J. Mol. Sci.20(22): 5626.

Bai CZ, Feng ML, Hao XL, Zhong QM, Tong LG and Wang ZH, 2015. Rutin, quercetin, and free amino acid analysis in buckwheat (Fagopyrum) seeds from different locations. Genet. Mol. Res.14: 19040–19048.

Bell CR, Pelly VS, Moeini A, Chiang SC, Flanagan E, Bromley CP, Clark C, Earnshaw CH, Koufaki MA, Bonavita E and Zelenay S, 2022. Chemotherapy-induced COX-2 upregulation by cancer cells defines their inflammatory properties and limits the efficacy of chemoimmunotherapy combinations. Nat. Commun. 13(1): 2063.

Berbecka M, Forma A, Baj J, Furtak-Niczyporuk M, Maciejewski R and Sitarz R, 2021. A systematic review of the cyclooxygenase-2 (COX-2) expression in rectal cancer patients treated with preoperative radiotherapy or radiochemotherapy. Curr. Issues Mol. Biol. 10(19): 4443.

Bhat SS, Prasad SK, Shivamallu C, Prasad KS, Syed A, Reddy P, Cull CA and Amachawadi RG, 2021. Genistein: A potent anti-breast cancer agent. Curr. Issues Mol. Biol. 43(3): 1502–1517.

Brown JS, Amend SR, Austin RH, Gatenby RA, Hammarlund EU and Pienta KJ, 2023. Updating the definition of cancer. Mol. Cancer Res. 21: 1142–1147.

Čermák V, Dostál V, Jelínek M, Libusová L, Kovář J, Rösel D and Brábek J, 2020. Microtubule-targeting agents and their impact on cancer treatment. Eur. J. Cell Biol. 99: 151075.

Cheng HS, Yip YS, Lim EKY, Wahli W and Tan NS, 2021. PPARγ and tumor microenvironment: the emerging roles of the metabolic master regulators in tumor stromal–epithelial crosstalk and carcinogenesis. Cancers (Basel) 13: 2153

Chunmei Z and Shuai W, 2025. Molecular mechanisms of neuroprotective effect of rutin. Front. Pharmacol. 16: 1599167.

Cimino-Mathews A, 2021. Novel uses of immunohistochemistry in breast pathology: interpretation and pitfalls. Mod. Pathol. 34: 62–77.

Daneshvar S, Zamanian MY, Ivraghi MS, Golmohammadi M, Modanloo M, Kamiab Z, Pourhosseini SME, Heidari M and Bazmandegan G, 2023. A comprehensive view on the apigenin impact on colorectal cancer. Food Sci. Nutr. 11(11): 6789–6801.

Dixit S, 2014. Anticancer effect of rutin isolated from the methanolic extract of Triticum aestivum straw in mice. Med. Sci. (Basel) 2: 153–160.

Dupain C, Ali HM, Mouhoub TA, Urbinati G and Massaad-Massade L, 2016. Induction of TTF-1 or PAX-8 expression on proliferation

and tumorigenicity in thyroid carcinomas. Int. J. Oncol. 49: 1248-1258.

Duffy MJ, Shering S, Sherry F, McDermott E and O'Higgins N, 2000. CA 15-3: a prognostic marker in breast cancer. Int. J. Biol. Markers 15: 330–333.

El Barky AR, Mohamed TM and Ali EMM, 2020. Detoxifying and antioxidant effect of ellagic acid nanoparticles in rats intoxicated with sodium nitrites. Appl. Biol. Chem. 63: 47.

Elbeltagi S, Mansour S, El-Tohamy HM, Ismail AM, Abdelbased KM, Alanazi MA, Al-Theyab NS and Eldin ZE, 2025. Apoptosis induction and anti-inflammatory cytokine effects of sorafenib-loaded MXene-UiO-66@liposome nanocomposites in liver cancer under NIR irradiation. Diam. Relat. Mater. 113092.

Ellman M, 1959. A spectrophotometric method for determination of reduced glutathione in tissues. Anal. Biochem. 74: 214–226.

Enogieru AB, Haylett W, Hiss DC, Bardien S and Ekpo OE, 2018. Rutin as a potent antioxidant: implications for neurodegenerative disorders. Oxid. Med. Cell. Longev. 2018: 6241017.

Fischer AH, Jacobson KA, Rose J and Zeller R, 2008. Hematoxylin and eosin staining of tissue and cell sections. In: Royer TAJ and Burns RB (eds.), CSH Protoc. Cold Spring Harbor Laboratory Press, Cold Spring Harbor, NY, USA.

Flaherty RL, Intabli H, Falcinelli M, Bucca G, Hesketh A, Patel BA, Allen MC, Smith CP and Flint MS, 2019. Stress hormone-mediated acceleration of breast cancer metastasis is halted by inhibition of nitric oxide synthase. Cancer Lett. 459: 59–71.

Ganeshpurkar A and Saluja AK, 2017. The pharmacological potential of rutin. Saudi Pharm. J. 25: 149–164.

Gasior A, Gorniak J, Voss A, Howard K, Harrison M, Gough L, Rollinson S and Pounce Z, 2025. Abstract P5-08-29: Assessment of RNA extraction protocols from FFPE breast cancer samples with the APIS breast cancer subtyping kit. Clin. Cancer Res. 31: 8–29.

Glorieux C, Sandoval JM, Dejeans N, Nonckreman S, Bahloula K, Poirel HA and Calderon PB, 2018. Evaluation of potential mechanisms controlling the catalase expression in breast cancer cells. Oxid. Med. Cell. Longev. 2018: 5351967.

Gopalakrishna R, Oh A, Hou L, Lee E, Aguilar J, Li A and Mack WJ, 2023. Flavonoid quercetin and its glucuronide and sulfate conjugates bind to 67-kDa laminin receptor and prevent neuronal cell death induced by serum starvation. Biochem. Biophys. Res. Commun. 671: 116–123.

Gorbushin AK, Luzan NA, Kakhanova VD, Koshmanova AA, Grek DS, Voronkovskii II, Farniev VM, Melikhova ES, Lukyanenko KA,Veprintsev DV and Morozov EV, 2025. Drug-induced partial immunosuppression for preclinical human tumor xenograft models. Cancers 17(24): 4025.

Gul S, Naseem M, Sheikh IS, Ali HM, Rabbani I, Jamil T, Gul S, Chachar Z, Ullah S, Asif S, Ataya FS, Fouad D, Abass KS, Cai Y, Liu J and Huang F, 2026. Troxerutin, a herbal metabolite with antidiabetic and antihypercholesterolemic potential, regulates metabolic gene activity in male diabetic rats. Front. Pharmacol. 16: 1687575.

Hajimehdipoor H, Tahmasvand Z, Ghorban Nejad F, Maresca M and Rajabi S, 2023. Rutin promotes proliferation and orchestrates epithelial–mesenchymal transition and angiogenesis in MCF-7 and MDA-MB-231 breast cancer cells. Nutrients 15(13): 2884.

Hammer A and Diakonova M, 2024. Prolactin-activated PAK1 potentiates estrogen response to breast cancer cell epithelial–mesenchymal transition, migration and invasion. In: Royer TAJ and Burns RB (eds.), microPubl. Biol. microPublication Press, Pasadena, USA.

He Y, Gu T, Cheng X, Yang Y, Li J, Zhai H, Chen M, Cao C, Li W, Wang S and Wang J, 2026. Diagnosis of axillary lymph node metastasis in breast cancer: a systematic review and meta-analysis of ultrasound and MRI studies published from 2014 to 2025. Quant. Imaging Med. Surg. 16(1): 15.

Huo M, Xia A, Cheng W, Zhou M, Wang J, Shi T, Cai C, Jin W, Zhou M, Liao Y and Liao Z, 2022. Rutin promotes pancreatic cancer cell apoptosis by upregulating miRNA-877-3p expression. Molecules 27(7): 2293.

Hussain R, Naz S, Alam S, Ali HM, Ali A, Khan MS, Fouad D, Ataya FS, Mammadov A and Li K, 2025. Temporal and dosage impact of magnesium oxide nanoparticles on grass carp:

unveiling oxidative stress, DNA damage, and antioxidant suppression. Toxicol. Mech. Methods 35(1): 19–31.

Jayatilleke KM and Hulett MD, 2020. Heparanase and the hallmarks of cancer. J. Transl. Med. 18: 453.

Jayatilleke KM, Duivenvoorden HM, Ryan GF, Parker BS and Hulett MD, 2023. Investigating the role of heparanase in breast cancer development utilising the MMTV-PyMT murine model of mammary carcinoma. Cancers 15(11): 3062.

Kim J, Harper A, McCormack V, Sung H, Houssami N, Morgan E, Mutebi M, Garvey G, Soerjomataram I and Fidler-Benaoudia MM, 2025. Global patterns and trends in breast cancer incidence and mortality across 185 countries. Nat. Med. 31(4): 1154–1162.

Kavarthapu R and Dufau ML, 2022. Prolactin receptor gene transcriptional control, regulatory modalities relevant to breast cancer resistance and invasiveness. Front. Endocrinol. (Lausanne) 13: 949396.

Keshaviah A, Dellapasqua S, Rotmensz N, Lindtner J, Crivellari D, Collins J, Colleoni M, Thürlimann B, Mendiola C and Aebi S, 2007. CA15-3 and alkaline phosphatase as predictors for breast cancer recurrence: a combined analysis of seven International Breast Cancer Study Group trials. Ann. Oncol. 18: 701–708.

Li Q, Qin M, Liu P and Liu M, 2026. Rutin alleviates pirarubicin-induced cardiotoxicity and enhances chemosensitivity in breast cancer. Phytomedicine 157818.

Lin JP, Yang JS, Lin JJ, Lai KC, Lu HF, Ma CY, Wu RSC, Wu KC, Chueh FS and Wood WG, 2012. Rutin inhibits human leukemia tumor growth in a murine xenograft model in vivo. Environ. Toxicol. 27: 480–484.

Liu Q, Pan R, Ding L, Zhang F, Hu L, Ding B, Zhu L, Xia Y and Dou X, 2017. Rutin exhibits hepatoprotective effects in a mouse model of non-alcoholic fatty liver disease by reducing hepatic lipid levels and mitigating lipid-induced oxidative injuries. Int. Immunopharmacol. 49: 132–141.

Magaki S, Hojat SA, Wei B, So A and Yong WH, 2019. An introduction to the performance of immunohistochemistry. In: Royer TAJ and Burns RB (eds.), Methods Immunohistochem. Springer, Berlin, Germany, pp. 289–298.

Maugeri A, Calderaro A, Patanè GT, Navarra M, Barreca D, Cirmi S and Felice MR, 2023. Targets involved in the anti-cancer activity of quercetin in breast, colorectal and liver neoplasms. Int. J. Mol. Sci. 24: 2952.

Mehra R, Varambally S, Ding L, Shen R, Sabel MS, Ghosh D, Chinnaiyan AM and Kleer CG, 2005. Identification of GATA-3 as a breast cancer prognostic marker by global gene expression meta-analysis. Cancer Res. 65: 11259–11264.

Molyneux G, Gibson FM, Chen CM, Marway HK, McKeag S, Mifsud CV, Pilling AM, Whayman MJ and Turton JA, 2008.The haemotoxicity of azathioprine in repeat-dose studies in the female CD-1 mouse. Int. J. Exp. Pathol. 89: 138–158.

Mukherjee P, Madsen CS, Ginardi AR, Tinder TL, Jacobs F, Parker J, Agrawal B, Longenecker BM and Gendler SJ, 2003. Mucin 1-specific immunotherapy in a mouse model of spontaneous breast cancer. J. Immunother. 26(1): 47–62.

Nishida A and Andoh A, 2025. The role of inflammation in cancer: mechanisms of tumor initiation, progression, and metastasis. Cells, 14: 488.

Nouhi Z, Chughtai N, Hartley S, Cocolakis E, Lebrun J-J and Ali S, 2006. Defining the role of prolactin as an invasion suppressor hormone in breast cancer cells. Cancer Res. 66: 1824–1832.

Plumb JA, 2004. Cell sensitivity assays: the MTT assay, pp. 165–169. In: Royer, TAJ & Burns, RB (eds.), Cancer Cell Culture: Methods and Protocols. Springer, New York, USA.

Rasheed M, Zaman MA, Zafar A, Khan MA, Anjum S, Ali HM, Hussain S, Zafar M, Yasin J, Hussain R and Ali A, 2024. Prophylactic effects of methylene blue, coconut and olive oils supplements on hemato-biochemical and histopathological parameters against p-phenylenediamine toxicity in male albino rats. Pak. Vet. J. 44(3): 840-846

Rathod NB, Elabed N, Punia S, Ozogul F, Kim SK and Rocha JM, 2023. Recent developments in polyphenol applications on human health: a review with current knowledge. Plants (Basel) 12: e 12061217

Reuter S, Gupta SC, Chaturvedi MM and Aggarwal BB, 2010. Oxidative stress, inflammation, and cancer: how are they linked? Free Radic. Biol. Med. 49: 1603–1612.

Riaz A, Ilan N, Vlodavsky I, Li JP and Johansson S, 2013. Characterization of heparanase-induced phosphatidylinositol 3-kinase AKT activation and its integrin dependence. J. Biol. Chem. 288(17): 12366–12375.

Satari A, Ghasemi S, Habtemariam S, Asgharian S and Lorigooini Z, 2021. Rutin: a flavonoid as an effective sensitizer for anticancer therapy; insights into multifaceted mechanisms and applicability for combination therapy. Evid. Based Complement. Alternat. Med. 2021: 9913179.

Schmittgen TD and Livak KJ, 2008. Analyzing real-time PCR data by the comparative CT method. Nat. Protoc. 3: 1101–1108.

Schuler LA and O'Leary KA, 2022. Prolactin: the third hormone in breast cancer. Front. Endocrinol. (Lausanne) 13: 910978.

Sicking I, Rommens K, Battista MJ, Böhm D, Gebhard S, Lebrecht A, Cotarelo C, Hoffmann G, Hengstler JG and Schmidt M, 2014. Prognostic influence of cyclooxygenase-2 protein and mRNA expression in node-negative breast cancer patients. BMC Cancer 14: 952.

Sikandar A, Zaneb H, Nasir A, Adil M, Ali HM, Muhammad M, Rehman T, Rehman A and Rehman HF, 2020. Bacillus subtilis on performance, immune system and gut in Salmonella-challenged broilers. S. Afr. J. Anim. Sci. 50(5): 654–662.

Singh BN, Shankar S and Srivastava RK, 2011. Green tea catechin epigallocatechin-3-gallate (EGCG): mechanisms, perspectives and clinical applications. Biochem. Pharmacol. 82(12): 1807–1821.

Smeda M, Kieronska A, Adamski MG, Proniewski B, Sternak M, Mohaissen T, Przyborowski K, Derszniak K, Kaczor D and Stojak M, 2018. Nitric oxide deficiency and endothelial–mesenchymal transition of pulmonary endothelium in the progression of 4T1 metastatic breast cancer in mice. Breast Cancer Res. 20: 86.

Sun X, Zhang G, Nian J, Yu M, Chen S, Zhang Y, Yang G, Yang L, Cheng P, Yan C, Ma Y, Meng H, Wang X and Li JP, 2017. Elevated heparanase expression is associated with poor prognosis in breast cancer: a study based on systematic review and TCGA data. Oncotarget 8(26): 43521–43535.

Tejwan N, Sadhukhan P, Sharma A, Singh TA, Hatimuria M, Pabbathi A, Das J and Sil PC, 2022. pH-responsive and targeted delivery of rutin for breast cancer therapy via folic acid functionalized carbon dots. Diam. Relat. Mater. 129: 109346.

Tian Y, Liu YR, Jin HZ, Lin QX, Zhao WY, Song WW, Gong YN, Deng YT, Wang SS, Wang K and Tian L, 2026. Catalase inhibits tumor growth by alleviating oxidative stress and promoting the polarization of tumor-associated macrophages from M2 to M1 phenotype in non-small cell lung cancer. Biol. Direct 21: 24.

Tobar-Delgado E, Mejía España D, Osorio Mora O and Serna Cock L, 2023. Rutin: family farming products' extraction sources, industrial applications and current trends in biological activity protection. Molecules 28: 5864.

Traverso N, Ricciarelli R, Nitti M, Marengo B, Furfaro AL, Pronzato MA, Marinari UM and Domenicotti C, 2013. Role of glutathione in cancer progression and chemoresistance. Oxid. Med. Cell. Longev. 2013: 972913.

Uti DE, Atangwho IJ, Alum EU, Ntaobeten E, Obeten UN, Bawa I, Agada SA, Ukam CI and Egbung GE, 2025. Antioxidants in cancer therapy mitigating lipid peroxidation without compromising treatment through nanotechnology. Discov. Nano 20: 70.

Urbinati G, de Waziers I, Slamiç M, Foussignière T, Ali HM, Desmaële D, Couvreur P and Massaad-Massade L, 2016. Knocking down TMPRSS2-ERG fusion oncogene by siRNA could be an alternative treatment to flutamide. Mol. Ther. Nucleic Acids 5.

Uygur MM and Gümüş M, 2021. The utility of serum tumor markers CEA and CA15-3 for breast cancer prognosis and their association with clinicopathological parameters. Cancer Treat. Res. Commun. 28: 100402.

Vodovotz Y, 1996. Modified microassay for serum nitrite and nitrate. Biotechniques 20: 390–394.

Wang X, Gong M, Zhu Z, Zhang B, Han L, Li W, Wu Z, Ma Q, Wang Z and Qian W, 2025. Rutin

protects the pancreas from inflammatory injury and oncogene-driven tumorigenesis by inhibiting acinar to ductal metaplasia. Eur. J. Pharmacol. 998: 177536.

Wu ZY, Qiu KY, Gai YJ, Wu JH, Zhou BX and Shi QF, 2025. Quercetin: a natural ally in combating breast cancer. Int. J. Nanomedicine 20: 9155–9177.

Xu J, Yuan X and Lang P, 1997. Determination of catalase activity and catalase inhibition by ultraviolet spectrophotometry. Chin. Environ. Chem. 16: 73–76.

Yang YC, Lin HY, Su KY, Chen CH, Yu YL, Lin CC, Yu SL, Yan HY, Su KJ and Chen YL, 2012. Rutin attenuates the senescence effect in a D-galactose aging mouse model. Evid. Based Complement. Alternat. Med. 2012: 980276.

Youssef S, Ibrahim N, El Sonbaty S and El Din Ezz M, 2022. Rutin suppresses DMBA carcinogenesis in the breast through modulating IL-6/NF-κB, SRC1/HSP90 and ER-α. Nat. Prod. Commun. 17(9): 1–11.

Zhang WT, Zhang W, Zhong YJ, Lü QY and Cheng J, 2013. Impact of quercetin on the expression of heparanase in cervical cancer cells. Zhonghua Fu Chan Ke Za Zhi 48(3): 198–203.